Journal of Power Sources 186 (2009) 344–348

Contents lists available at ScienceDirect

Journal of Power Sources

journal homepage: www.elsevier.com/locate/jpowsour

Short communication

Synthesis and properties of $(La_{0.75}Sr_{0.25})_{0.95}MnO_{3\pm\delta}$ nano-powder prepared via Pechini route

Jian Xin Wang, You Kun Tao, Jing Shao, Wei Guo Wang*

Division of Fuel Cell and Energy Technology, Ningbo Institute of Material Technology & Engineering, Chinese Academy of Sciences, Ningbo 315201, PR China

ARTICLE INFO

Article history:
Received 4 September 2008
Received in revised form
26 September 2008
Accepted 30 September 2008
Available online 17 October 2008

Keywords:
Nanocrystalline powders
Lanthanum manganate composite cathode
Polarization resistance

ABSTRACT

$(La_{0.75}Sr_{0.25})_{0.95}MnO_{3\pm\delta}$ (LSM) powders have been synthesized via a Pechini route. The prepared powders were characterized by XRD, SEM, XRF, BET and particle size distribution (PSD) analysis. It is shown that the morphology and structure of the oxide particles are significantly dependent on the preparation conditions such as the sort of surfactant and pH value of the starting solution. High purity, single phase, homogeneous, nanocrystalline LSM powders with slight aggregation were obtained using citric acid as complexing agent, ethylene glycol as surfactant and pH 1. The conductivity of the sintered LSM sample prepared from this nanocrystalline powders was mensurated about 200 S cm^{-1} in air at 600–1000 °C. The impedance spectra of symmetric cells LSM–YSZ/YSZ/LSM–YSZ were measured in air and open circuit voltage condition. The optimal polarization resistance (R_p) of 0.175 Ω cm^2 at 750 °C and 0.07 Ω cm^2 at 800 °C was obtained in the sample with LSM to YSZ weight ratio of 49:51.

1. Introduction

Due to the excellent power generation characteristics, planar anode-supported SOFCs with thin YSZ electrolyte lead the developments of intermediate-temperature SOFCs (operated between 650 °C and 800 °C) [1–4]. A typical anode-supported cell consists of Ni–YSZ cermets as anode, YSZ as electrolyte and LSM $(La_{0.75}Sr_{0.25})_{0.95}MnO_{3\pm\delta}$)–YSZ as cathode. The theoretical and experimental works have shown that in this type of cells, the YSZ film (around 10 μm in thickness) contributes a minor ohmic resistance. So, it becomes less necessary for the cell performance improvement through further reducing the electrolyte thickness. The State-of-the-art porous Ni–YSZ anode substrate also brings about negligible polarization loss, while the LSM–YSZ cathode loss dominates the total cell loss at 650–800 °C [1–4]. So enhancement of the cell performance at 800 °C or further reduction of the operation temperature to 600–750 °C can primarily be achieved by improving the LSM–YSZ cathode performance.

LSM–YSZ composite cathode was firstly reported by Kenjo and Nishiya [5]. The incorporation of electrolyte material in the cathode has shown to improve electrode performance at lower temperatures by increasing the volume of active sites available for electrochemical reactions. In the LSM–YSZ composite cathode, the electrochemical reduction of oxygen occurs at the conjunction of the three-phase boundaries (TPBs). The three phases are LSM, YSZ and gas pores. In a fuel cell using composite cathode, the TPBs extend well into the cathode in areas placed away from the physically distinct cathode/electrolyte interface, and substantially lower the cathodic polarization. Therefore not only the microstructure at the cathode/electrolyte interface, but also the entire cathode microstructure was considered to be responsible for the polarization of the cathode. Accordingly, LSM–YSZ composite electrodes have demonstrated better performance than those composed of only LSM. Now the addition of YSZ component to the cathode of an SOFC is a general method to enhance the electrochemical performance of the LSM-based system. To reduce the polarization resistance in the LSM–YSZ cathode, many groups have studied the relationship between the cathode microstructure and the electrochemical properties [6–10]. These studies have demonstrated that a composite cathode with desirable microstructure is the key to obtaining good electric and chemical performance of the cathode. At Risø National Laboratory, the processing optimization of the LSM–YSZ composite cathode was carried out in a systematic way, area specific polarization resistances (R_p) as low as 0.06 Ω cm^2 at 850 °C and 0.24 Ω cm^2 at 750 °C have been achieved using a nanostructure LSM–YSZ composite cathode, which has lead to an improved power density of 0.8 W cm^{-2} at 750 °C under 0.7 V for the anode-supported cells [3,11]. Their publication neither reported the detailed information of LSM powder synthesis nor LSM powder properties.

It is known that the electrical performances of an electrode are significantly dependent on their composition and microstructure.

* Corresponding author. Tel.: +86 574 8791 1363; fax: +86 574 8668 5139.
E-mail address: wgwang@nimte.ac.cn (W.G. Wang).

0378-7753/$ – see front matter © 2008 Elsevier B.V. All rights reserved.
doi:10.1016/j.jpowsour.2008.09.116

The homogeneous starting powder is prerequisite for the manufacture of high performance electrode, since the microstructure and properties of ceramics are significantly influenced by the characteristics of preliminary powder. Several preparation techniques based on the solid-state reaction and some solution chemistry methods, such as drip pyrolysis, citrate-gel process, sol–gel process [12] and co-precipitation technique [13] were developed to prepare the LSM powders. The LSM powders made by the solid-state reaction method usually have larger particle size and poorer catalytic activity than solution chemistry methods. Drip pyrolysis was proved to produce LSM powders with a poor surface area. The citrate-gel, sol–gel and co-precipitation routes as mentioned above can make the particle size smaller but the powders usually aggregate easily.

The aim of this study is to modify the Pechini route and make it suitable for preparing optimum LSM powders with large scale. The influence of preparation conditions such as the sort of surfactant, pH value of the starting solution on the structure and morphology of the LSM powders was studied. As-prepared LSM powders, LSM bulks and the LSM–YSZ symmetric samples were also studied.

2. Experimental

2.1. Powder synthesis and characterization

Nanocrystalline LSM powders were prepared by a modified sol–gel process using citric acid as complexing agent. This method is preferred to the traditional solid-state reaction method, because it can give rise to more homogeneous powders with controlled stoichiometry and microstructure. Briefly, $La(NO_3)_3$, $Sr(NO_3)_2$ and $Mn(NO_3)_2$ solutions with stoichiometric ratio $(La_{0.75}Sr_{0.25})_{0.95}MnO_{3\pm\delta}$ were prepared separately and mixed with gentle stirring. An adequate amount of citric acid was added to the mixtures. The mixtures were kept in a water bath at 80 °C with constant stirring for about 1 h, then an adequate amount of surfactant was added to boost the reaction. The pH of the solution was adjusted to the required level with the addition of nitric acid or ammonia solution. The precursor solution kept in a water bath at 80 °C until gelation was completed, and then the as-prepared gels were dried at 120 °C and 250 °C, respectively. The ultrafine LSM powders were obtained by calcining the dried gel at 800 °C for 5 h. In this study, three kinds of surfactant (PEG, PVA and EG) and pH value of 1 and 3 were used.

In the solid-state reaction route, LSM powders of the same composition was prepared by ball milling a mixture of La_2O_3, $SrCO_3$ and $MnCO_3$ powders in the required proportion. The milled powders were calcined at 1000 °C for 6 h in air.

These nanocrystalline powders were grounded by hand for about 1 h. Pressed bars of 25 mm × 8 mm × 3 mm were shaped by uniaxial pressing at a pressure of about 200 MPa, and then sintered at 1250 °C for 5 h. For comparison, LSM ceramic bulks were also synthesized with the powders prepared by solid-state reaction method at 1300 °C for 5 h.

Phase formation and crystallinity of the resulting powders were characterized by means of X-ray diffraction (XRD) in a Bruker D8 Advance with Cu Kα radiation. The microstructures of the LSM powders and sintered samples were observed by field emission scanning electron microscope (FESEM, Sirion 200 FEG). The purity of the synthesized LSM powders was measured by XRF (Rigaku ZSX Primus II). Specific surface areas of LSM powders were measured by the Brunauer–Emmett–Teller (BET) isotherm technique with nitrogen adsorption using a Micromeritics ASAP 2020M physisorption analyzer. Particle size distribution (PSD) analysis was made by Zatasizer nano ZS Malvern Instruments Ltd. (UK). The electrical conductivity of the sintered LSM samples was measured by four-probe DC measurement in the temperature range of 25–1000 °C in air.

2.2. Symmetric cell fabrication and measurement

The LSM powders with the nominal compositions $(La_{0.75}Sr_{0.25})_{0.95}MnO_{3\pm\delta}$ have been produced by the modified sol–gel process. The YSZ component in the composite electrodes is a commercial powder, TZ-8Y (ZrO2 with 8 mol% Y_2O_3, Tosoh Corporation). An ethanol-based slurry of LSM and YSZ was produced by ball milling and sprayed on both sides of an approximately 200 μm thick YSZ foil using airborne spraying. The cells were sintered at 1000 °C for 2 h. The sintered cells were painted with platinum paste and cut to dimensions of 7.1 mm × 7.1 mm. The tests were performed as two-electrode four-wire measurements, and the polarization resistance was determined as half of the measured electrode polarization resistance [3,11,14]. Impedance measurements were carried out using a Solartron 1260 frequency response analyzer over the frequency range from 2 MHz to 0.1 Hz and 20 mV excitation voltage at 650–850 °C in air. The microstructure of the symmetric cells was investigated using the FESEM (Hitachi S-4800). In this study, LSM–YSZ samples with LSM to YSZ weight ratio of 46:54, 47:53, 49:51, 50:50, 51:49 and 52:48 were prepared and labeled as sample LSM46, LSM47, LSM49, LSM50, LSM51 and LSM52, respectively.

3. Results and discussion

3.1. Results of LSM powders research

The XRD patterns of the LSM powders prepared using different surfactants and pH values are shown in Fig. 1. All powder samples were calcined at 800 °C for 5 h. For three kinds of powders with pH 1, only the XRD patterns of crystalline $La_{0.74}Sr_{0.26}MnO_3$ (PDF Number: 00-056-0616) were observed, while for three kinds of powders with pH 3, besides $La_{0.74}Sr_{0.26}MnO_3$ phase, the presence of $SrCO_3$ phase was observed in the XRD patterns. It suggests that a precursor solution with pH 1 seems to favor the chelation between metal ions and citric acid and facilitate the crystallization. The pH value of the solution has an evident effect on the chelating process, while the sort of surfactant has a neglectable effect on the crystallization of the LSM powder. The crystallite size of the powders prepared in this study was about 20 nm as deduced from the XRD pattern by Debye–Scherer equation after subtraction of the equipment widening.

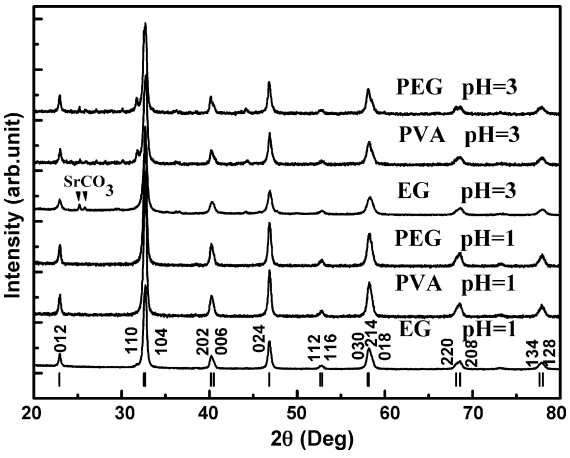

Fig. 1. XRD patterns of LSM powders prepared from different conditions.

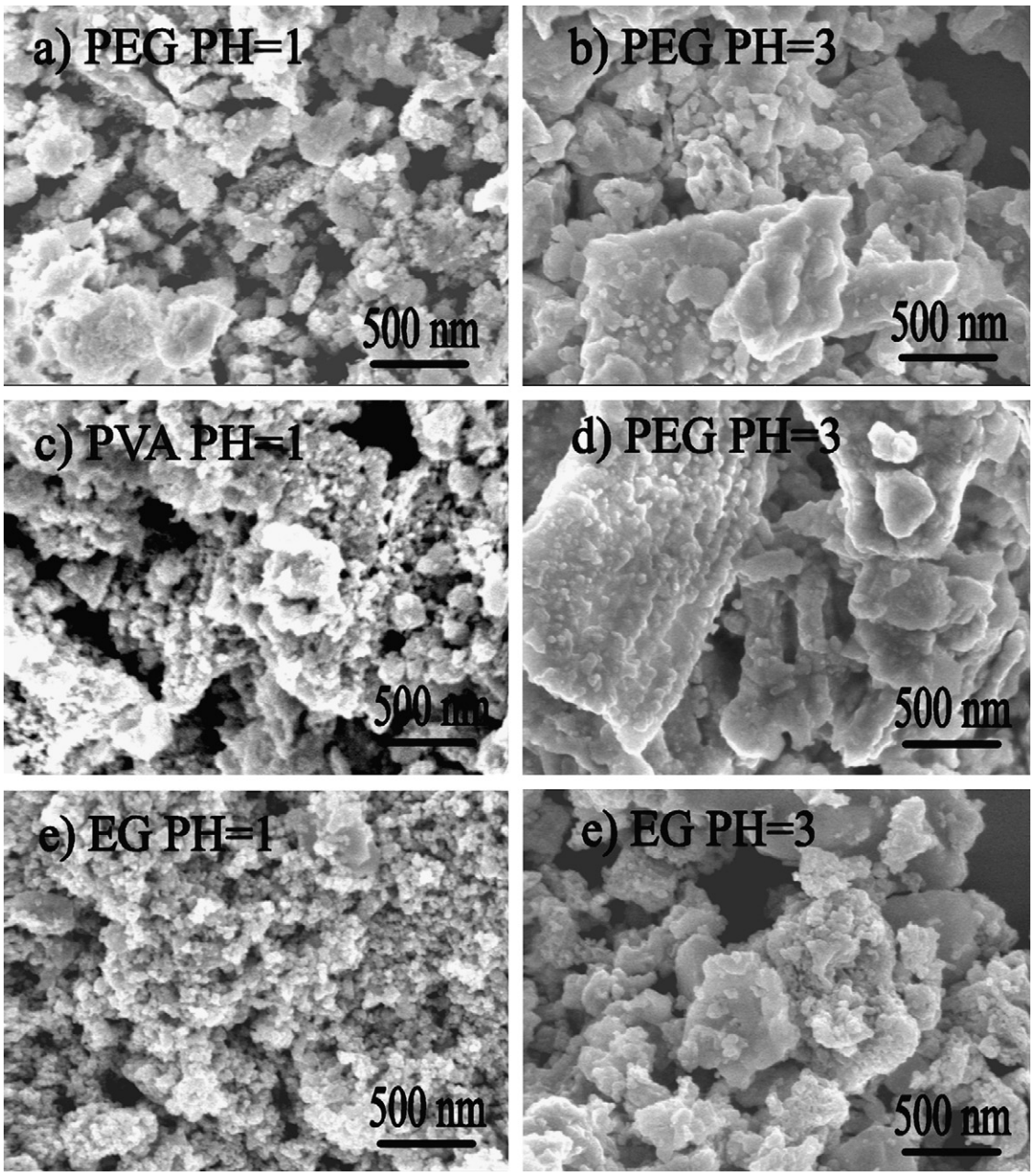

Fig. 2. SEM pictures of LSM powders prepared from different conditions.

The SEM images shown in Fig. 2 correspond to six kinds of LSM powders prepared from the different surfactants and pH values. The microstructures of powders are significantly dependent on both the sort of surfactant and the pH value. Clearly, only the LSM powders in Fig. 2(e) have few aggregates, and the particle size is less than 100 nm with a narrow distribution. While a lot of distinct aggregates appear in the other powders. It is obvious that the morphology of the LSM particles is significantly dependent on the preparation conditions.

As a whole, the optimization conditions of prepared the LSM powders are using citric acid as complexing agent, ethylene glycol as surfactant and pH 1. This modified sol–gel process is also called the Pechini method and has been used before in Ref. [12].

Furthermore, this preparation process was scaled up to a capacity of 110 g powders per cycle, the LSM powders as-prepared were characterized by XRF, BET and PSD analysis. The XRF results show that the LSM powders are composed of La_2O_3 55.0 wt%, MnO 32.7 wt% and SrO 12.2 wt%, which indicated that the powders composition is near the nominal $(La_{0.75}Sr_{0.25})_{0.95}MnO_{3\pm\delta}$, the purity of the LSM powders is higher than 99.9%. The special surface area of the LSM powders is found to be 14.8 $m^2\ g^{-1}$ at the calcination temperature of 800 °C. PSD analysis shows that the particle size of LSM powders is around 100–200 nm with a narrow distribution.

In view of all characterizations of the LSM powders, it can be concluded that the process optimization has lead a high purity, single phase, homogeneous and slight aggregation LSM powders with grain size 50–80 nm.

3.2. Electrical conductivity of the LSM bulk

Fig. 3 shows the electrical conductivity of the sintered LSM samples from the nanocrystalline powders and from microcrystalline

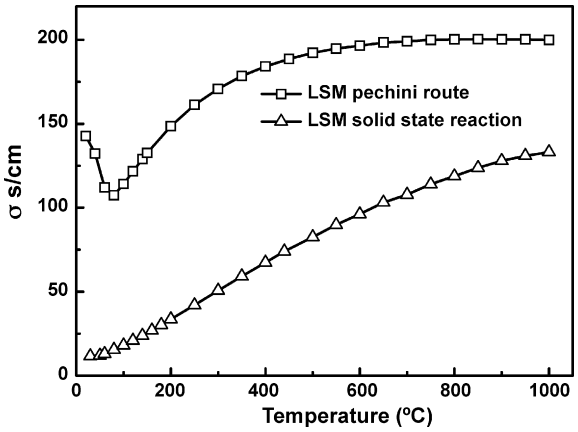

Fig. 3. The electrical conductivity of the sintered LSM samples.

powders prepared by solid-state reaction method. The sample sintered from the nanocrystalline powders exhibits a high electronic conductivity almost 200 S cm^{-1}, while the conductivity of sample prepared by solid-state reaction method is only around 100 S cm^{-1} in the temperature range 600–1000 °C. Electronic conductivity of pure $La_{0.7}Sr_{0.3}MnO_3$ bulk synthesized by a modified amorphous citrate process was reported as 110 S cm^{-1} in air at 800 °C [15].

The high conductivity of the sample sintered from the LSM nanocrystalline powders could be attributed to the excellent performance of nanocrystalline powders. The performances of nanocrystalline powders are more superior than the common powders fabricated by conventional solid-state reaction. The nanocrystalline powders can provide faster densification kinetics, lower sintering temperatures, and better mechanical and electrical properties. Furthermore, it seems that the process of the chemical preparation of nanocrystalline powders will result in higher purity of the samples than in the normal solid-state reaction method preparation of microcrystalline powders.

3.3. Symmetric cell measurement

The electrochemical properties of the symmetrical cells of LSM–YSZ cathode were studied and the typical impedance spectra are given in Fig. 4. A series of R_p and R_s were extracted from the curves according to the indications shown in the spectra.

Fig. 5 shows the Arrhenius plot of the R_p obtained from the impedance spectra of all LSM–YSZ samples. For comparison, the results reported in Ref. [3] are showed in this figure too. By carefully adjusting LSM content in the LSM–YSZ composites from 46% to 52%, low area specific polarization resistance of 0.175 Ω cm^2 at 750 °C and 0.07 Ω cm^2 at 800 °C have been achieved in symmetric cells with the LSM content 49%. The volume ratio of LSM to YSZ is more important than the weight ratio in the electrode. The weight ratio of LSM:YSZ = 49:51 converted to volume ratio is about 47.4:52.6. This performance indicates that the anode-supported cell with improved LSM–YSZ composite cathode has the potential to be operated at 700–750 °C with an acceptable power density.

Fig. 6 displays the fracture cross-section morphology of the symmetric cell, LSM49. The LSM–YSZ coat was about 20 μm thick and has a very fine structured composite with uniformly distributed LSM, YSZ and pores. The individual grains are clear and round. The grain size is approximately of 200 nm. Because the backscattered coefficients of LSM and YSZ are very close to each other, the two phases cannot be distinguished clearly in Fig. 6. However, energy dispersive spectrometry EDS mapping as shown in Fig. 7 shows

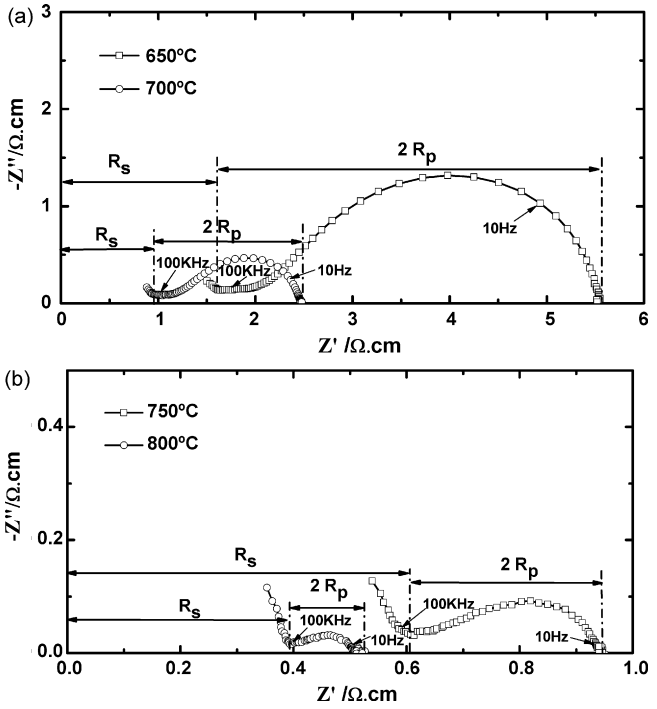

Fig. 4. Typical impedance spectra of the LSM49 symmetric cell obtained in air and open circuit voltage (OCV) condition for different temperatures. The area of the cell is approximately 0.71 cm × 0.71 cm.

that the distribution of the LSM, YSZ grains and pores is homogeneous. Sintering necks between the grains indicate good connection between LSM/LSM, LSM/YSZ or YSZ/YSZ grains. The LSM and YSZ were sintered together forming a network, and it was incorporated uniformly with a network of pores. The YSZ network provides the channels for carrying oxygen farther into the composite LSM–YSZ electrode [16]. Furthermore, the LSM–YSZ coat is well adhered to the YSZ substrate. It can be seen that almost all the available "branches" of the LSM–YSZ network at the interfacial region are connected to the YSZ substrate. Such connected network offers large extended contacts between ionic conductor electrolyte YSZ and electronic conductor LSM. Porous structure with very small grain size enlarges the number of the active TPBs [11]. Good electric and chemical performance is believed to be related to such homo-

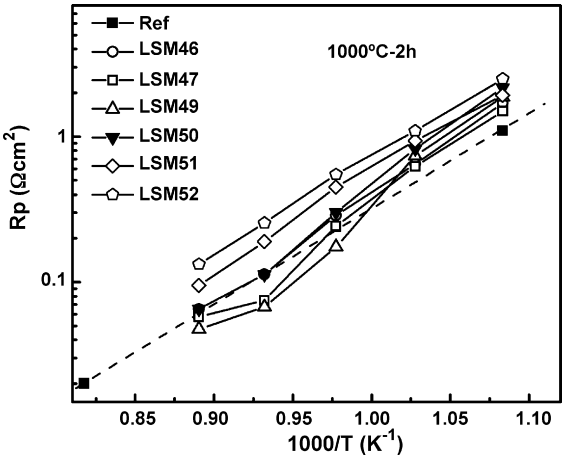

Fig. 5. Arrhenius plot of the cathode area specific polarization resistance, R_p obtained from impedance measurements in air and open circuit voltage (OCV) condition.

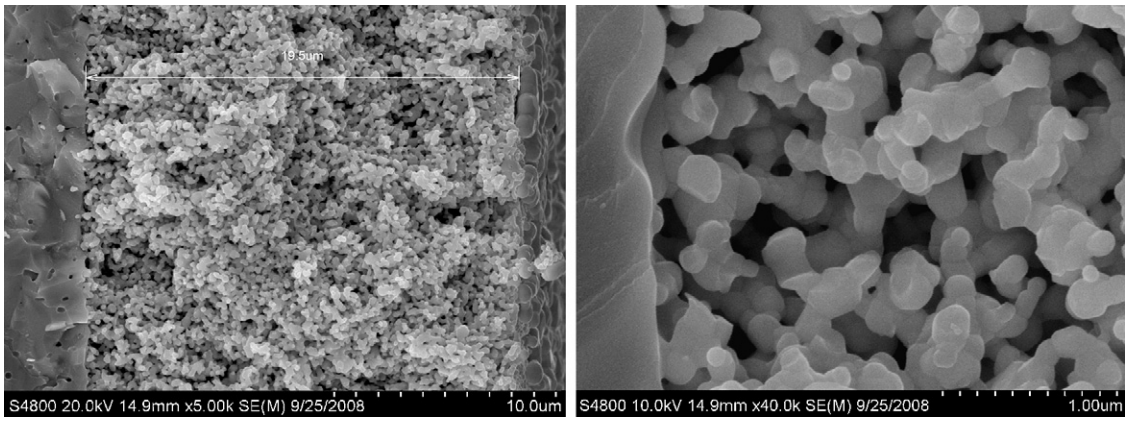

Fig. 6. SEM pictures of the cross-section for the symmetric cell, LSM49.

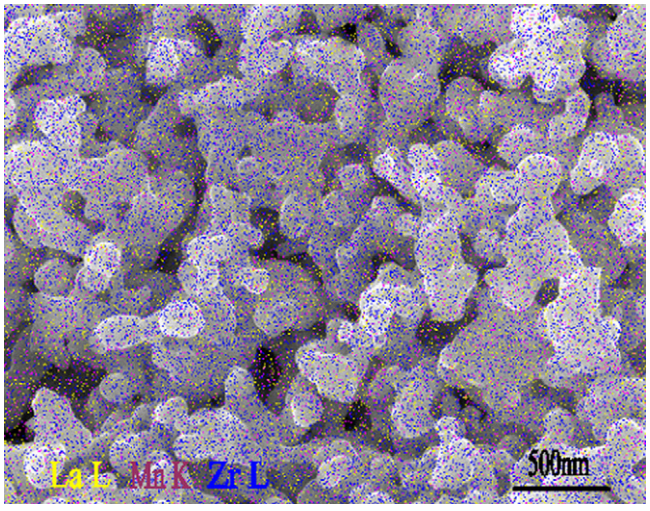

Fig. 7. EDS mapping of the cross-section for the symmetric cell, LSM49.

geneous porous composite nanostructure, which can increase the length of the active TPBs, thereby lower the cathodic polarization.

4. Conclusions

Nanocrystalline $(La_{0.75}Sr_{0.25})_{0.95}MnO_{3\pm\delta}$ powders have been successfully synthesized by a Pechini route, the optimization conditions are using citric acid as complexing agent, ethylene glycol as surfactant and pH 1. Process optimization has lead a high purity, single phase, homogeneous and slight aggregation LSM powders with grain size 50–80 nm. The conductivity of the sintered LSM sample prepared from this nanocrystalline powders is mensurated about 200 S cm^{-1} in air at 600–1000 °C, which is almost double of the conductivity of the LSM sample prepared by solid-state reaction method. By carefully adjusting LSM content in the LSM–YSZ composites, a performance with R_p of 0.07 Ω cm^2 at 800 °C and less than 0.2 Ω cm^2 at 750 °C in symmetric cells with the configuration of LSM–YSZ/YSZ/LSM–YSZ has been achieved. These results have indicated that the Pechini route is an excellent technique to synthesize LSM powders with a good performance. This work has also demonstrated that LSM–YSZ cathode with low cathodic polarization can be achieved by the homogeneous porous composite nanostructure.

Acknowledgements

This work is partly supported by the National High Technology Research and Development Program of China (863 Program, Grant No. 2007AA05Z140) and Chinese Academy of Sciences.

References

[1] S.D. Souza, S.J. Visco, L.C.D. Jonghe, J. Electrochem. Soc. 144 (1997) L35.
[2] J.-W. Kim, A.V. Virkar, K.-Z. Fung, K. Mehta, S.C. Singhal, J. Electrochem. Soc. 146 (1999) 69.
[3] W.G. Wang, R. Barfod, P.H. Larsen, K. Kammer, J.J. Bentzen, P.V. Hendriksen, M. Mogensen, in: S.C. Singhal, M. Dokiya (Eds.), Solid Oxide Fuel Cells VIII, PV 2003-07, The Electrochemical Society Proceedings Series, Pennington, NJ, 2003, p. 400.
[4] Z. Wang, M. Cheng, Y. Dong, M. Zhang, H. Zhang, Solid State Ionics 176 (2005) 2555–2561.
[5] T. Kenjo, M. Nishiya, Solid State Ionics 57 (1992) 295.
[6] J.H. Choi, J.H. Jang, J.H. Ryu, S.M. Oh, J. Power Sources 87 (2000) 92–100.
[7] S.P. Yoon, J. Han, S.W. Nam, T.-H. Lim, I.-H. Oha, S.-A. Hong, Y.-S. Yoo, H.C. Lim, J. Power Sources 106 (2002) 160–166.
[8] T. Suzuki, M. Awano, P. Jasinski, V. Petrovsky, H.U. Anderson, Solid State Ionics 177 (2006) 2071–2074.
[9] V.A.C. Haanappel, J. Mertens, D. Rutenbeck, C. Tropartz, W. Herzhof, D. Sebold, F. Tietz, J. Power Sources 141 (2005) 216–226.
[10] H.S. Song, W.H. Kim, S.H. Hyun, J. Moona, J. Kim, H.-W. Lee, J. Power Sources 167 (2007) 258–264.
[11] W.G. Wang, Y.-L. Liu, R. Barfod, S.B. Schougaard, P. Gordes, S. Ramousse, P.V. Hendriksen, M. Mogensen, Electrochem. Solid-State Lett. 8 (12) (2005) A619–A621.
[12] M. Gaudon, C. Laberty-Robert, F. Ansart, P. Stevens, A. Rousset, Solid State Sci. 4 (2002) 125–133.
[13] V. Uskokovic, M. Drofenik, Mater. Des. 28 (2007) 667–672.
[14] M.J. Jørgensen, S. Primdahl, M. Mogensen, Electrochim. Acta 44 (1999) 4195–4201.
[15] G.S. Godoi, D.P.F. de Souza, Mater. Sci. Eng. B 140 (2007) 90–97.
[16] W. Tanner, K.-Z. Fung, A.V. Virkar, J. Electrochem. Soc. 144 (1997) 21.